

INVESTIGATION OF A SHROUDED ROTOR-STATOR DISK CAVITY

Ram P. Roy, G. Xu, and J. Feng
Arizona State University
Tempe, Arizona



Gas Turbine Heat Transfer Laboratory,
Mechanical & Aerospace Engineering

**INVESTIGATION OF A SHROUDED ROTOR-STATOR
DISK CAVITY**

R. P. Roy, G. Xu and J. Feng

Arizona State University
Department of Mechanical and Aerospace Engineering
Tempe, AZ 85287-6106

*NASA Seal/Secondary Air System Workshop
October 25-26, 2000*

OBJECTIVES

TO UNDERSTAND:

1. TIME-AVERAGE AND UNSTEADY PRESSURE FIELDS IN THE MAIN-STREAM GAS PATH AND DISK CAVITY
2. VELOCITY FIELD IN THE MAIN GAS PATH AND DISK CAVITY
3. INGESTION OF MAIN GAS INTO THE DISK CAVITY
4. CONVECTIVE HEAT TRANSFER IN THE DISK CAVITY
5. EFFECTIVE RIM SEAL CONFIGURATIONS

APPROACH TAKEN:

EXPERIMENTS AND CFD SIMULATION

EXPERIMENTS PRESENTED

$\underline{\text{Re}}_\phi$	$\underline{\text{Re}}_m$	$\underline{\beta}$	\underline{c}_w	$\underline{c}_{w, \text{fd}}$
5.16×10^5	5.0×10^5	19.5°	0	8140
5.16×10^5	5.0×10^5	19.5°	1504	8140
5.16×10^5	5.0×10^5	19.5°	7520	8140

Re_m = main–stream flow Reynolds number, $= \rho V_m b / \mu$

Re_ϕ = disk rotational Reynolds number, $= \rho \Omega b^2 / \mu$

c_w = nondimensional mass flow rate of secondary air, $= \dot{m} / \mu b$

$c_{w, \text{fd}}$ = nondimensional free disk pumping mass flow rate, $= 0.219 \text{Re}_\phi^{0.8}$

CONVECTIVE HEAT TRANSFER AT ROTOR DISK SURFACE

Local convective heat transfer coefficient:

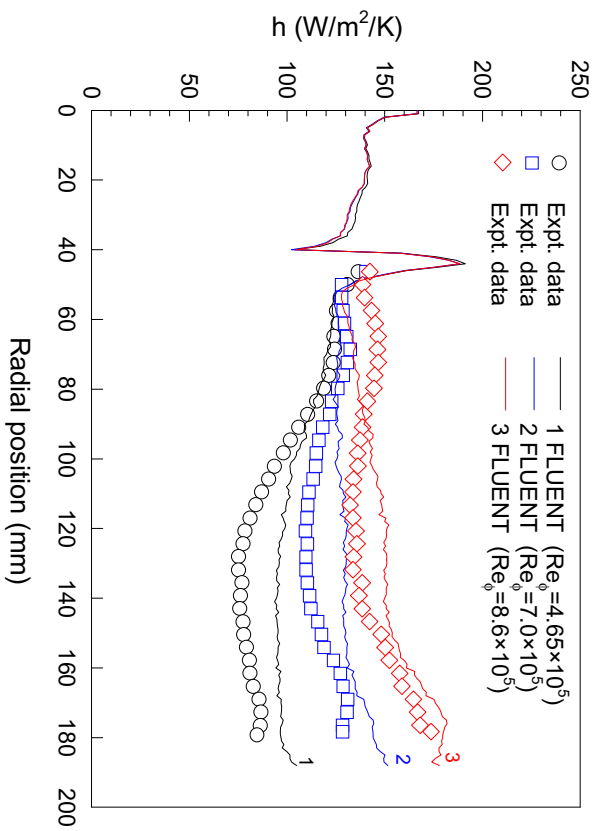
$$h(r) = \frac{q''_{w,ro,conv}(r)}{T_{w,ro} - T_{ref}(r)} = \frac{q''_{w,ro}(r) - q''_{w,ro,rad}}{T_{w,ro} - T_{ref}(r)}$$

Local Nusselt number:

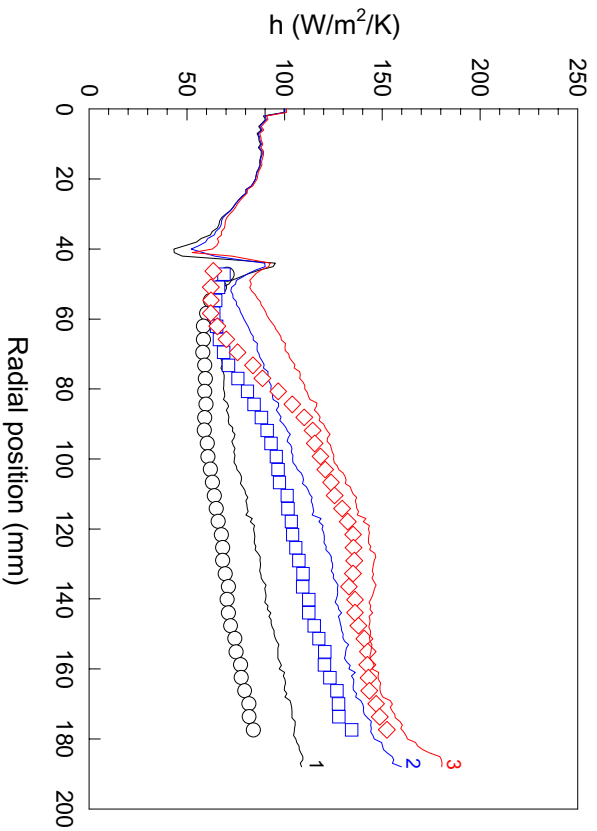
$$Nu_r \equiv \frac{h(r)r}{k_{air}}$$

Local rotational Reynolds number:

$$\text{Re}_{\phi,r} \equiv \frac{\rho \Omega^2 r^2}{\mu} = \left(\frac{r}{b}\right)^2 \text{Re}_{\phi}$$

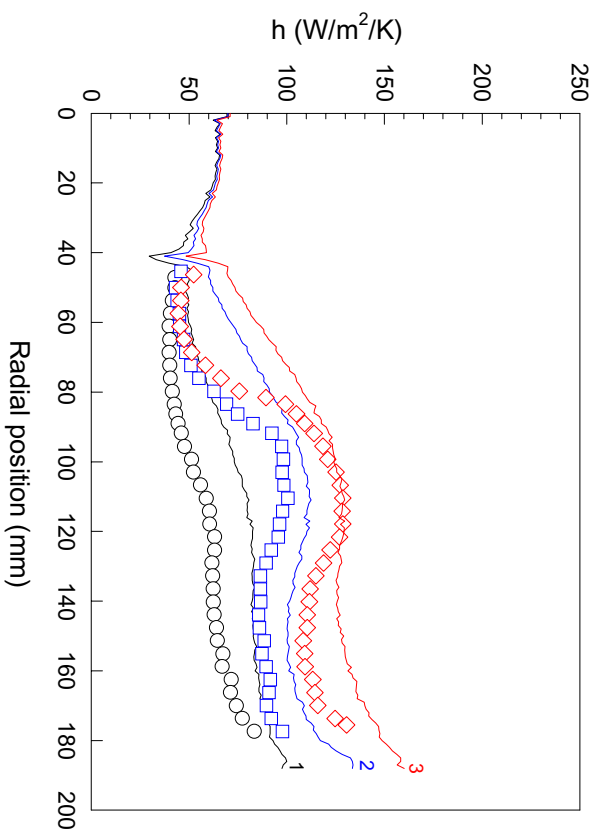


(a) $c_w = 7520$

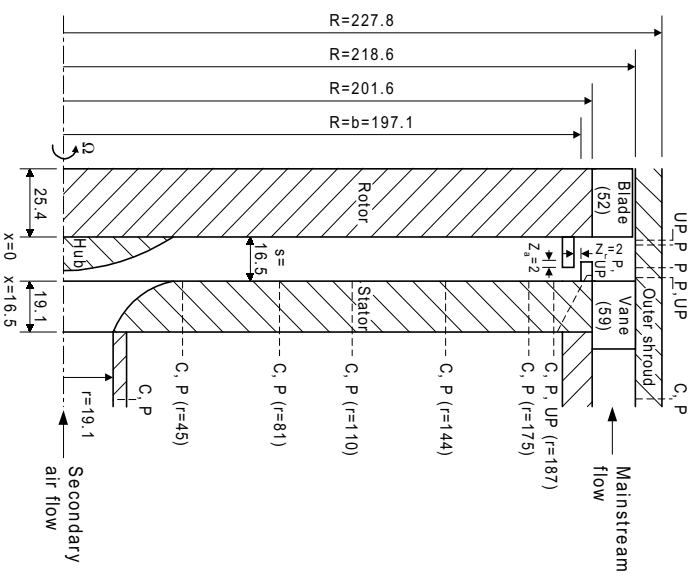


(b) $c_w = 3008$

Effect of rotor disk speed on the convective heat transfer coefficient distribution

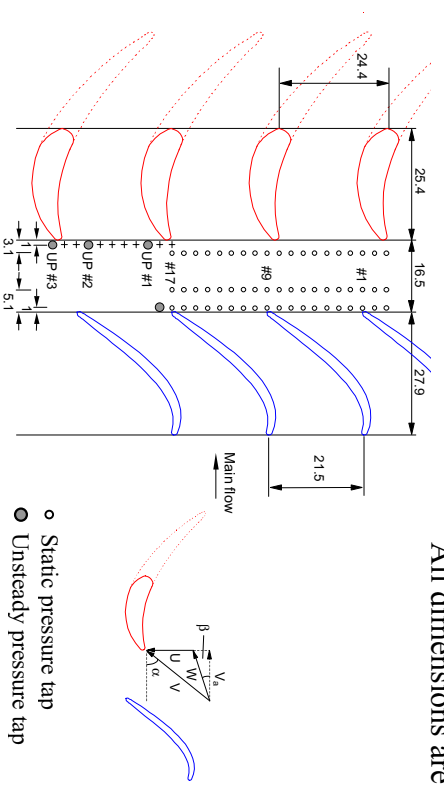


(c) $c_w=1504$



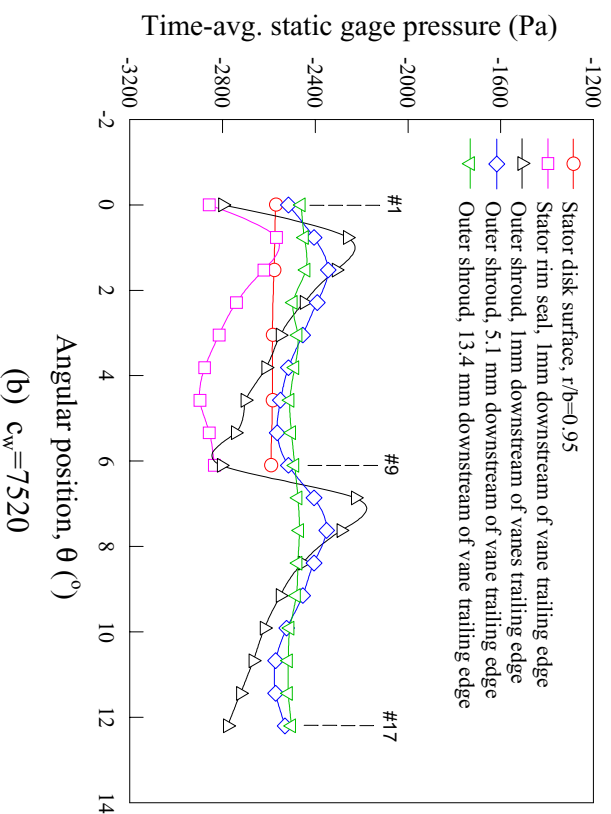
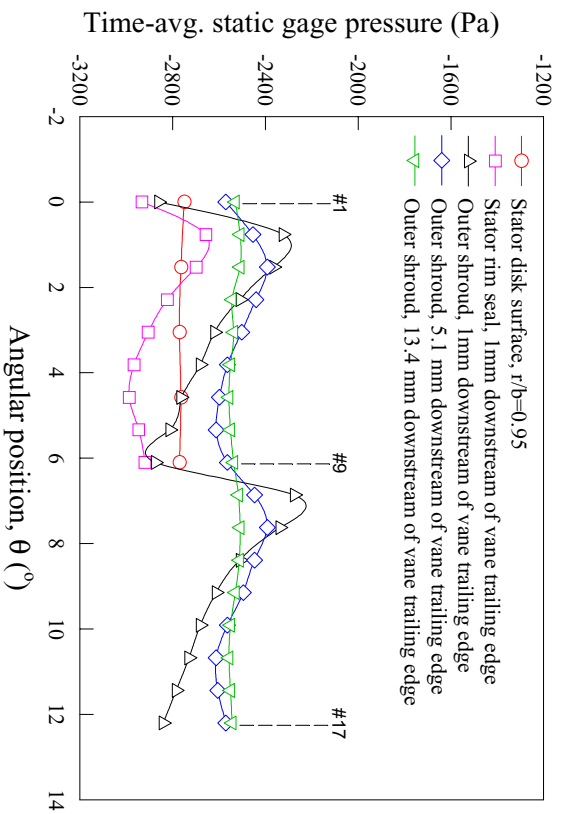
(a) The disk cavity

All dimensions are in mm

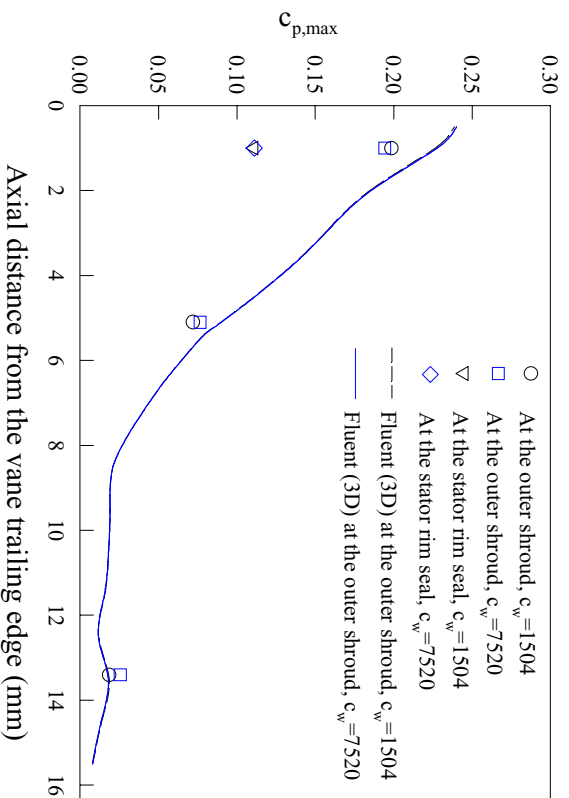


(b) Schematic of blades and vanes

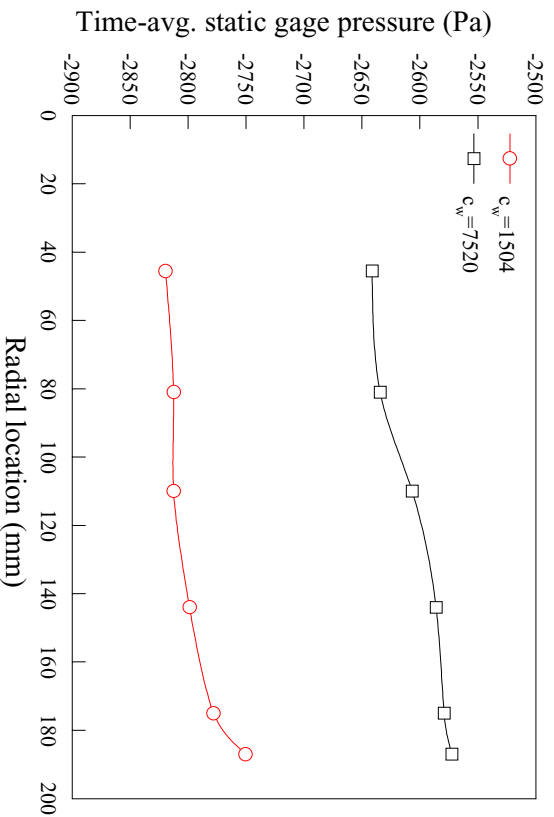
The rotor-stator system (C: tracer gas concentration tap, P: static pressure tap, UP: unsteady pressure tap)



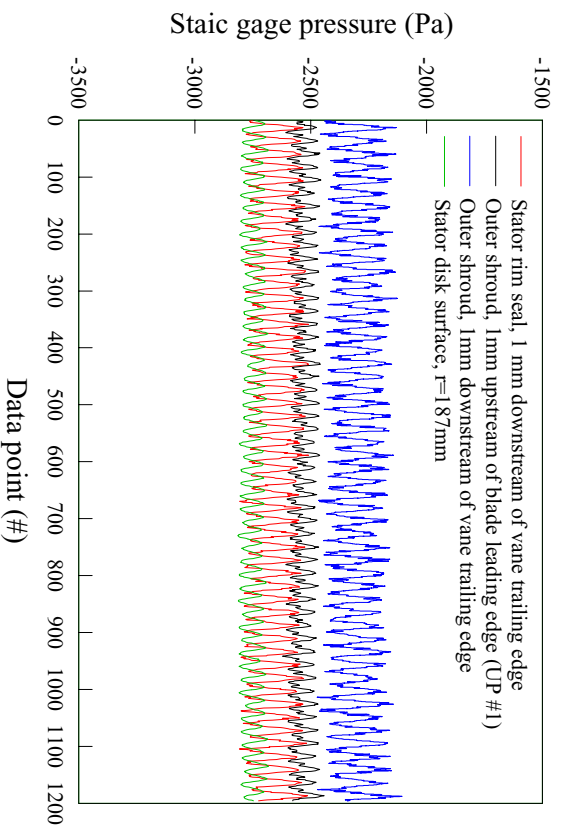
Measured circumferential distributions of time-average static pressure at the outer shroud, stator disk rim seal, and stator disk surface near its rim ($Re_{\phi}=5.16 \times 10^5$, $Re_m=5.0 \times 10^5$)



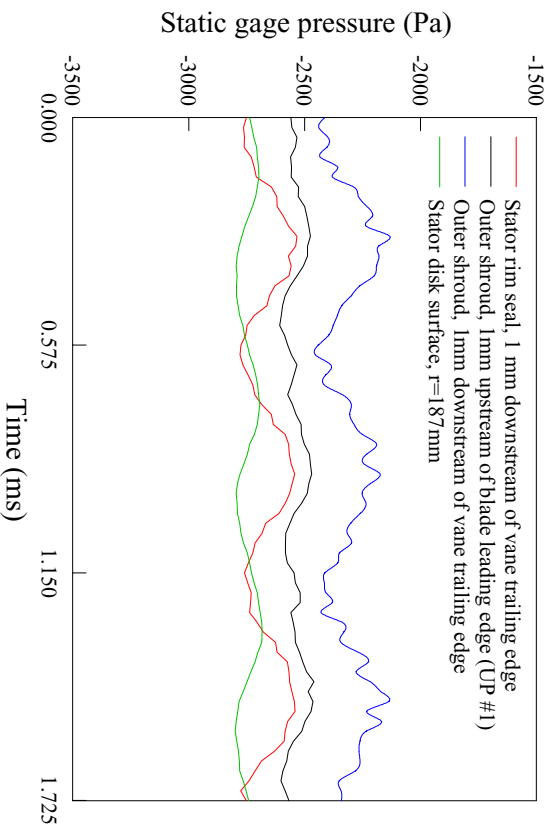
Time-average static pressure circumferential asymmetry coefficient at the main gas path outer shroud and stator rim seal ($Re_\phi=5.16 \times 10^5$, $Re_m=5.0 \times 10^5$)



Radial distribution of static pressure at the stator disk surface for two secondary air flow rates ($Re_\phi=5.16 \times 10^5$, $Re_m=5.0 \times 10^5$)

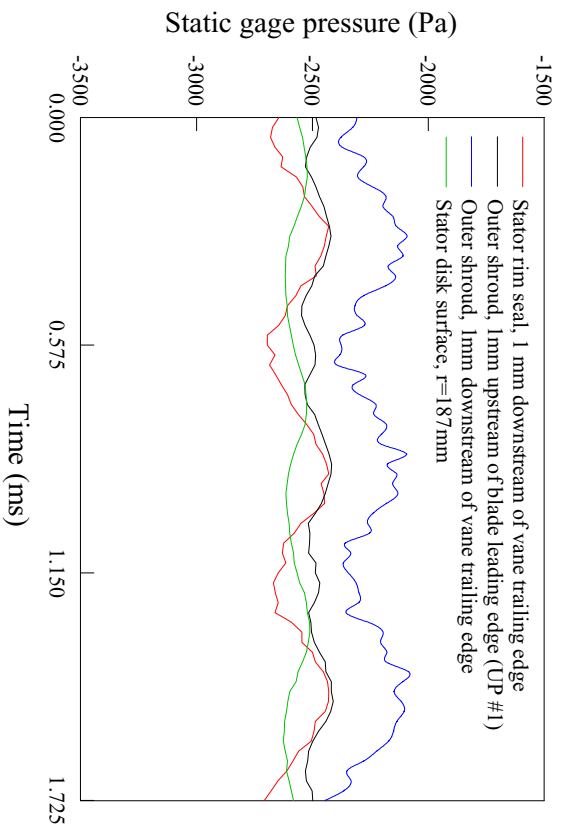


(a) $c_w=1504$ – one revolution of rotor disk

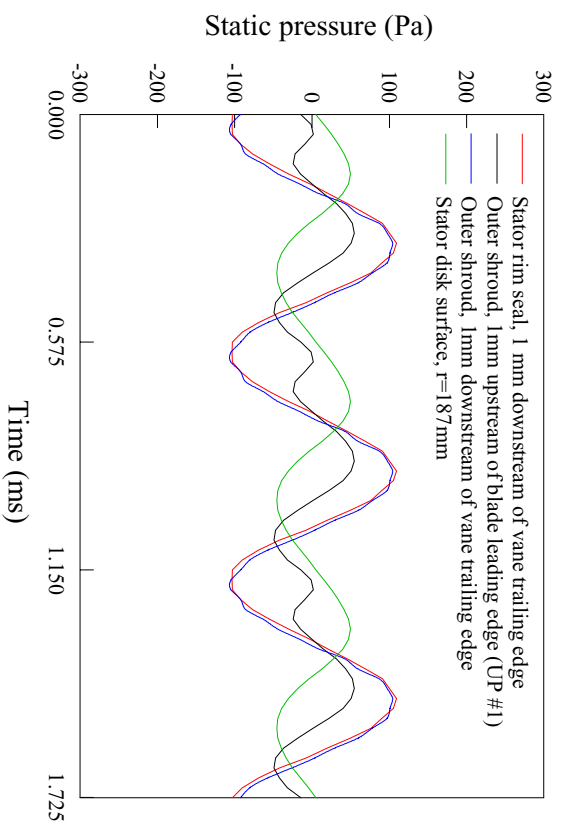


(b) $c_w=1504$ – three blade passages

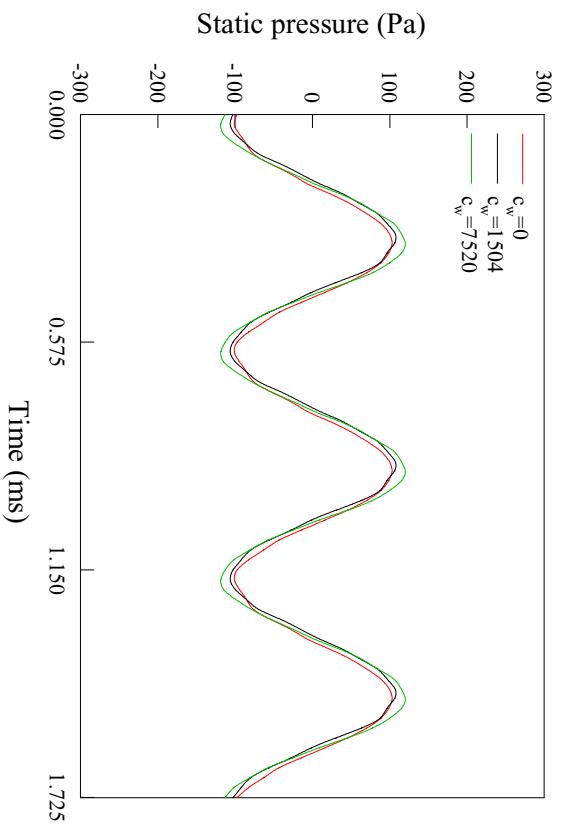
Ensemble-average unsteady static pressure at the outer shroud, rim seal of stator disk, and stator disk surface near the rim ($Re_\phi=5.16 \times 10^5$, $Re_m=5.0 \times 10^5$)



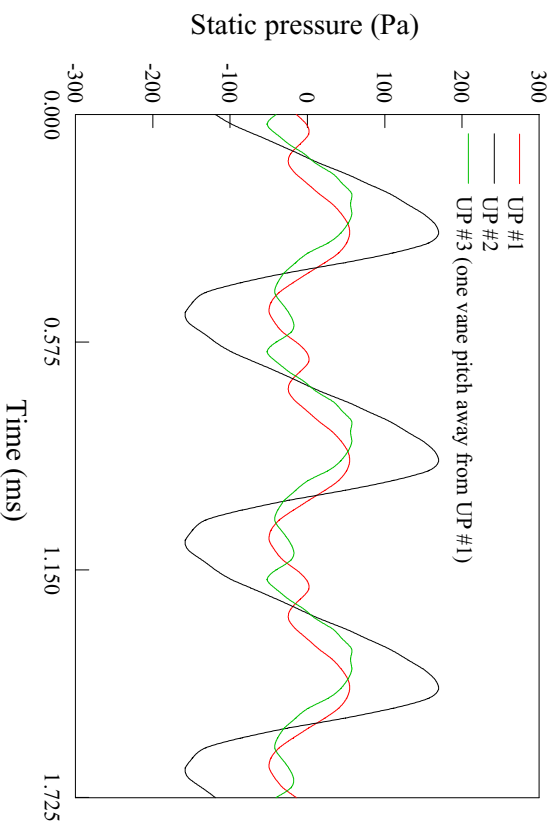
(c) $c_w=7520$ – three blade passages



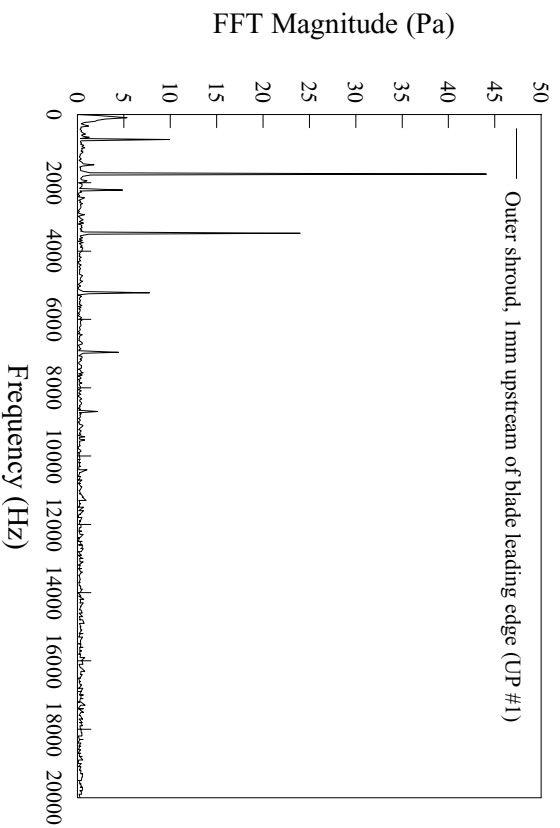
Blade–periodic static gage pressure at the outer shroud, stator disk rim seal, and stator disk surface near its rim ($Re_\phi=5.16\times 10^5$, $Re_m=5.0\times 10^5$, $c_w=1504$) – three blade passages



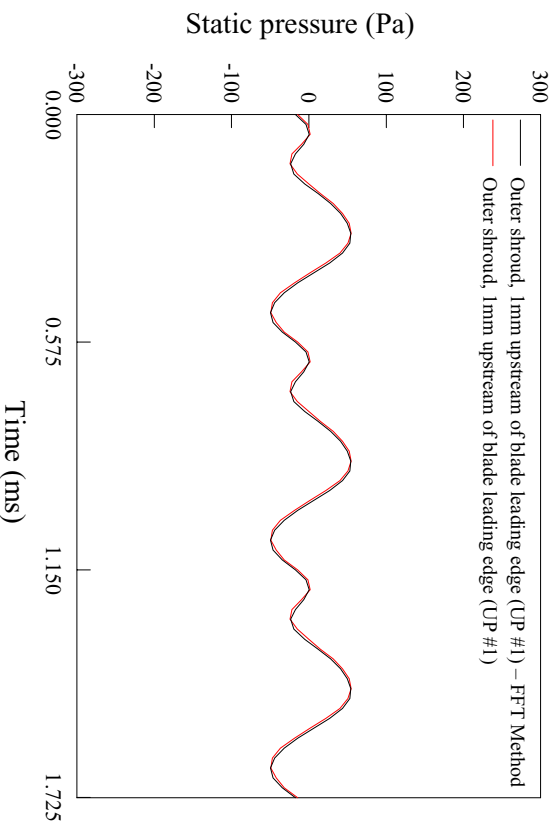
Effect of secondary air flow rate on blade-periodic static pressure at the stator disk rim seal 1 mm downstream of vane trailing edge ($Re_\phi = 5.16 \times 10^5$, $Re_m = 5.0 \times 10^5$) – three blade passages



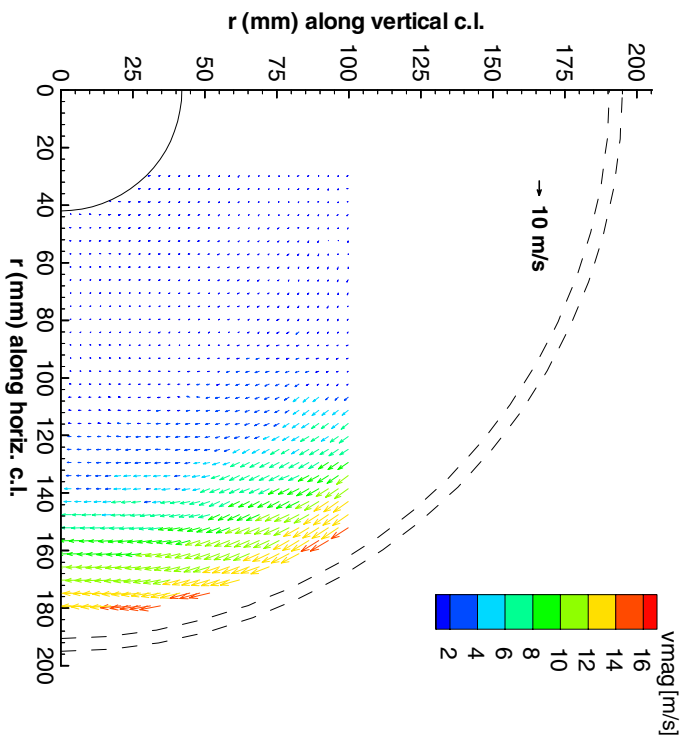
Circumferential variation of blade-periodic static pressure at the outer shroud 1 mm upstream of blade leading edge ($Re_\phi = 5.16 \times 10^5$, $Re_m = 5.0 \times 10^5$, $c_w = 1504$) – three blade passages



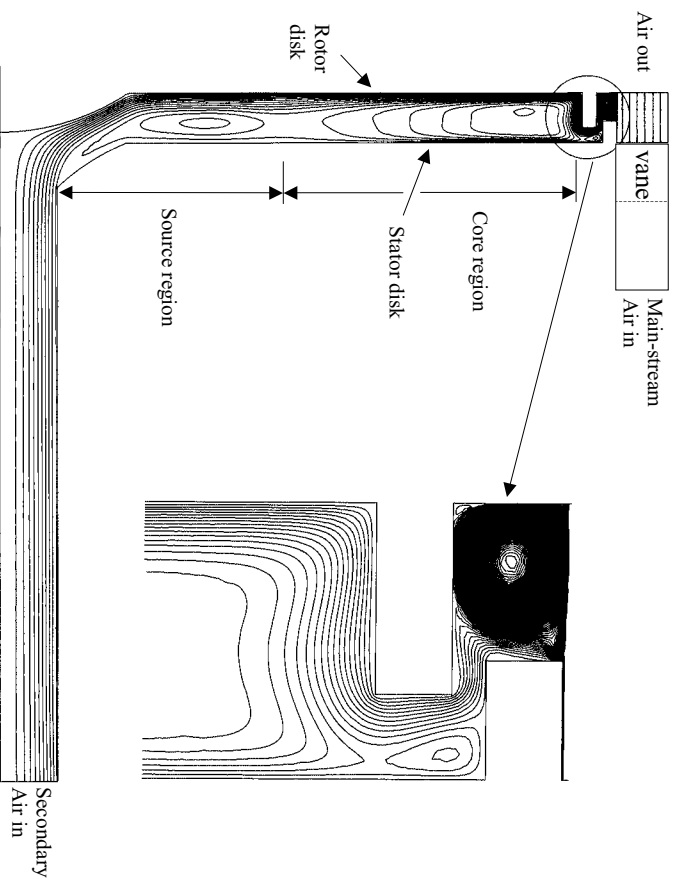
Frequency spectrum of the ensemble-average static pressure fluctuation at the outer shroud 1 mm upstream of blade leading edge ($Re_\phi=5.16 \times 10^5$, $Re_m=5.0 \times 10^5$, $c_w=1504$)



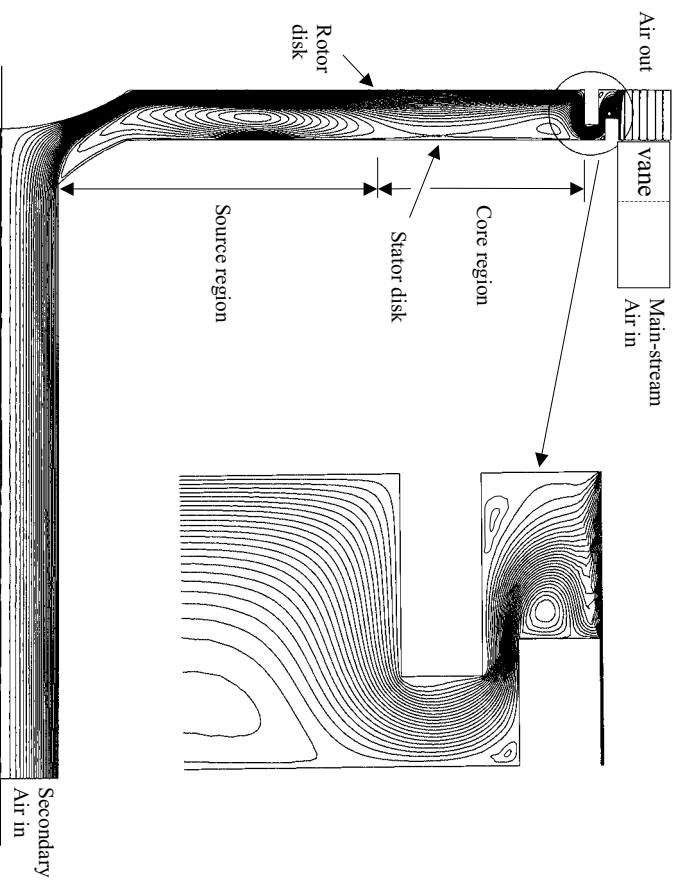
Comparison of FFT method with decomposition method: blade-periodic static pressure at the outer shroud 1 mm upstream of blade leading edge ($Re_\phi=5.16 \times 10^5$, $Re_m=5.0 \times 10^5$, $c_w=1504$) – three blade passages



r - ϕ plane map of the fluid time-average velocity in the cavity 3 mm from the stator disk
for $Re_\theta=5.16 \times 10^5$, $Re_m=5.0 \times 10^5$, $c_w=1504$

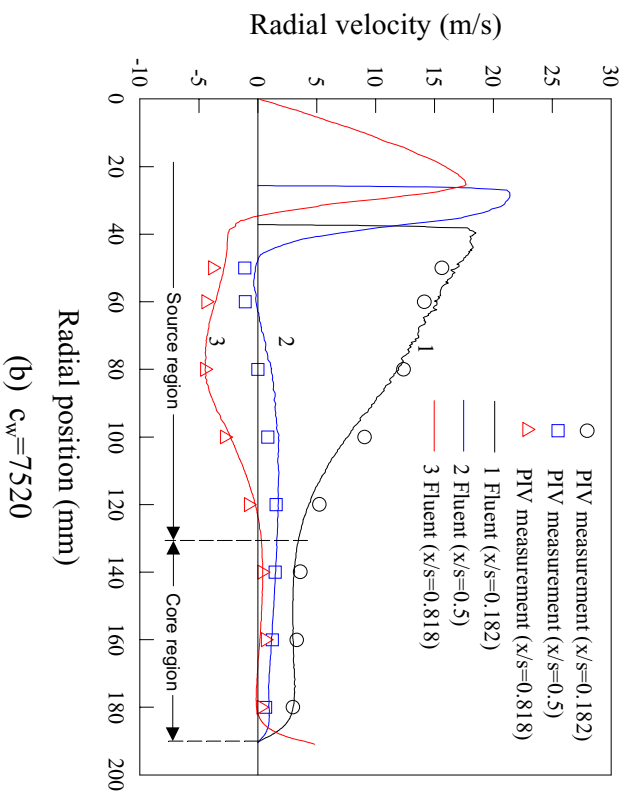
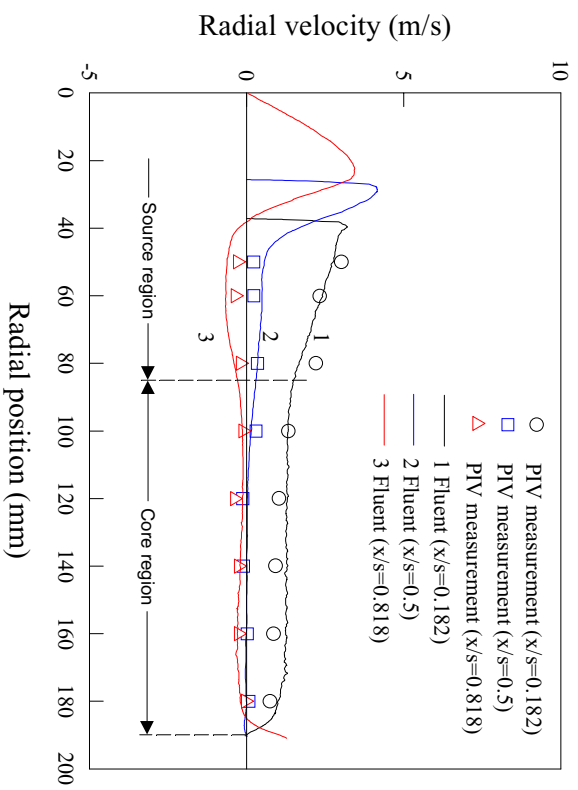


(a) $c_w = 1504$

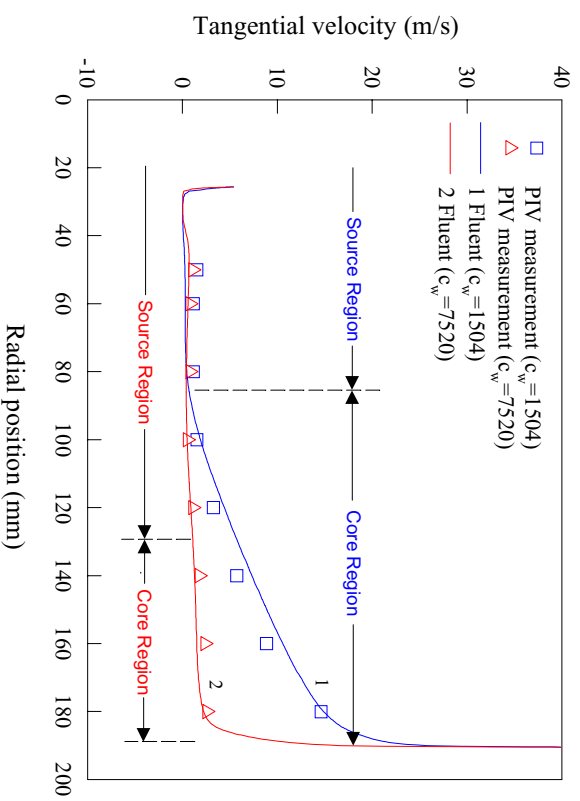


(b) $c_w = 7520$

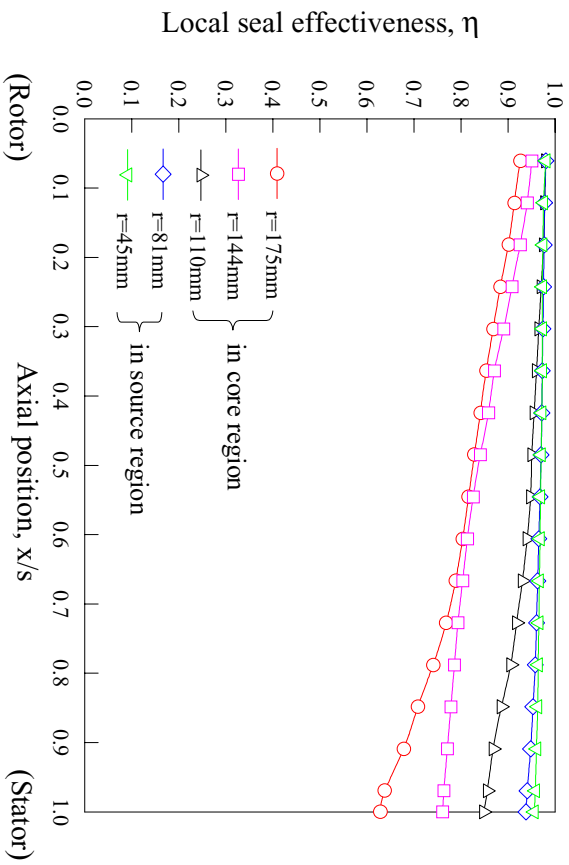
Computed streamlines for $Re_\theta = 5.16 \times 10^5$, $Re_m = 5.0 \times 10^5$
(steady rotationally-symmetric simulation)



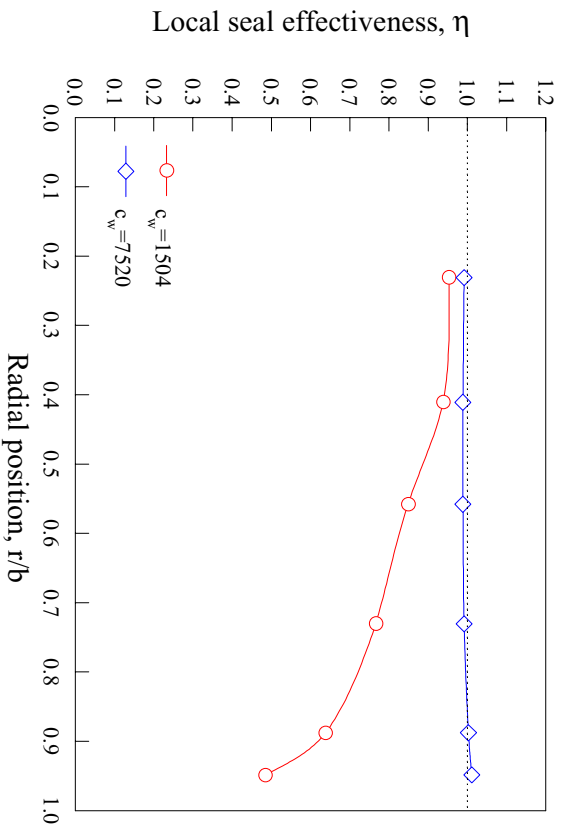
Radial distribution of fluid radial velocities at $Re_\phi=5.16 \times 10^5$, $Re_m=5.0 \times 10^5$



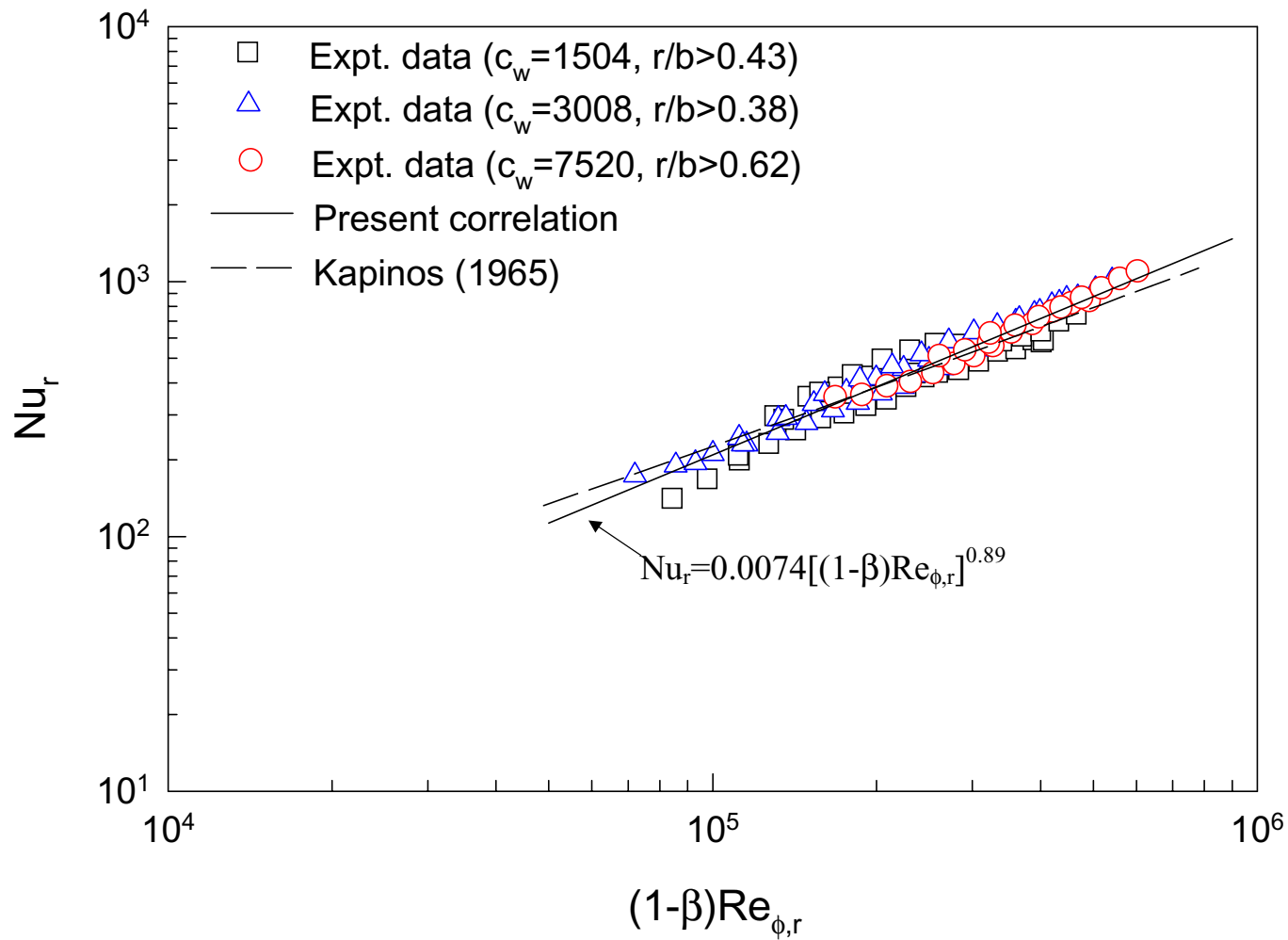
Effect of c_w on the fluid tangential velocity at the cavity mid-axial gap ($x/s=0.5$) for $Re_\theta=5.16 \times 10^5$, $Re_m=5.0 \times 10^5$



Seal effectiveness distribution in the disk cavity for $Re_\phi=5.16 \times 10^5$, $Re_m=5.0 \times 10^5$, $c_w = 1504$



Seal effectiveness distributions at the stator disk surface for $Re_\phi=5.16 \times 10^5$, $Re_m=5.0 \times 10^5$



Local Nusselt number versus local relative rotational Reynolds number (expt. data and correlation are for the core region and radially outermost part of the source region) – β , core fluid rotation ratio, = $V_\phi/\Omega r$